

# The LEAF picosecond pulse radiolysis facility at Brookhaven National Laboratory

James F. Wishart,<sup>a)</sup> Andrew R. Cook, and John R. Miller  
*Chemistry Department, Brookhaven National Laboratory, Upton, New York 11973-5000*

(Received 9 February 2004; accepted 14 July 2004; published 29 October 2004)

The BNL Laser-Electron Accelerator Facility (LEAF) uses a laser-pulsed photocathode, radio-frequency electron gun to generate  $\geq 7$  ps pulses of 8.7 MeV electrons for pulse radiolysis experiments. The compact and operationally simple accelerator system includes synchronized laser pulses that can be used to probe or excite the electron-pulsed samples to examine the dynamics and reactivity of chemical species on the picosecond time scale. © 2004 American Institute of Physics. [DOI: 10.1063/1.1807004]

## I. INTRODUCTION

Pulse radiolysis has been an important method for studying chemical kinetics in condensed and aqueous phases for 40 years.<sup>1</sup> Electron accelerators are the most common and convenient pulsed radiation sources for kinetic measurements.<sup>2</sup> Many electrostatic (e.g., Van de Graaff) and radio frequency (e.g., linac) accelerators with pulse widths on the order of a few nanoseconds are in use worldwide for pulse radiolysis. On the other hand, the number of pulse radiolysis facilities with time resolution shorter than one nanosecond is very small. The first radiolysis installation capable of resolving picosecond time scale kinetics was developed at the University of Toronto in the late 1960s.<sup>3(a),3(b)</sup> It took advantage of the fine structure of  $\sim 30$  ps pulses contained within the 30 ns envelope of the accelerator macropulse. The stroboscopic transient detection system used optically delayed Cerenkov radiation generated by the individual electron bunches to probe transients created by later bunches within the macropulse. The Toronto instrument opened a new time regime for radiolysis studies, which led to many important findings on reactions within spurs.

During the 1970s and 1980s, pulse radiolysis facilities based on single-electron-bunch linear accelerators with pulse widths on the order of picoseconds were constructed at Argonne National Laboratory (Illinois),<sup>3(c)</sup> at the University of Tokyo Nuclear Engineering Research Laboratory (NERL) in Tokai-mura, Japan,<sup>4</sup> and at Osaka University (Japan).<sup>5</sup> All three installations used a grid-gated thermionic cathode to inject electrons into a radio frequency prebunching section operating at a subharmonic of the accelerator frequency.<sup>2</sup> The subharmonic prebuncher compresses the electron bunch until it can be inserted into the linac section within a single period of the accelerator frequency. After acceleration, magnetic compression is sometimes used to reduce the pulse width from 30 ps to 0.2–5 ps.<sup>6</sup> In addition to the linear accelerator facilities, a Van de Graaff-based system in Delft, Netherlands, generates subnanosecond pulses.<sup>7</sup>

Within the last 15 years a new type of electron accelera-

tor capable of producing picosecond pulses has been developed, based on the radio-frequency photocathode electron gun.<sup>8</sup> A rf photocathode gun consists of two to four resonant cavities filled with high microwave power to produce field gradients on the order of 60–100 MV/m. The first cell of the gun (usually a half-cell) incorporates a back plate with a photocathode surface such as copper or magnesium metal or a semiconductor such as cesium telluride ( $\text{Cs}_2\text{Te}$ ). A laser pulse is timed to generate photoelectrons when the accelerating gradient is optimal, resulting in acceleration of the electron bunch to energies of 4–9 MeV within a few tens of centimeters. Electron bunches with charges of several nanocoulombs and pulse widths on the order of picoseconds are obtained by using picosecond laser excitation with pulse energies up to several hundred microjoules. The electron gun may be coupled to further acceleration sections to produce a higher energy beam.<sup>9</sup> Photocathode electron guns produce beams with very clean position-momentum relationships that allow precision beam control for critical applications such as free-electron lasers.<sup>10</sup> The development of rf photocathode accelerators has been driven by applications like these and many such installations exist.

As the technology of rf photocathode guns began to develop, it was recognized that it offered the means to create a new type of picosecond pulse radiolysis facility with several potential advantages over first-generation facilities. Without the need for a subharmonic prebunching system and a conventional linac section, the accelerator would be much more compact, allowing one to build a smaller enclosure while leaving ample room for experimental installations. The microwave system would also be vastly simpler, without the need to amplify multiple frequencies and to control the relative phase of several rf sections. The inherent availability of picosecond-synchronized electron and laser beams at photocathode accelerator installations facilitates advanced experimental detection techniques such as electron pulse/laser probe transient absorption spectroscopy.

Encouraged by these prospects, a workshop<sup>11</sup> was held at Brookhaven National Laboratory in September 1989 to evaluate experimental needs and establish design criteria for a picosecond pulse radiolysis facility based on a rf photo-

<sup>a)</sup>Electronic mail: wishart@bnl.gov

cathode electron gun accelerator. Contemporaneously, rf photocathode gun development was occurring at the BNL Accelerator Test Facility (ATF), where a 1.5 cell gun (BNL Gun I) was built and tested.<sup>8(a)</sup> Collaboration between the BNL ATF and Grumman Aerospace Corporation (later Northrop-Grumman Corporation, now Advanced Energy Systems, Inc., Medford, NY) led to the design of a 3.5-cell gun (Gun II) capable of accelerating electrons to energies of 9 MeV.<sup>8(b)</sup> The Gun II design was adapted for the Grumman Compact Infrared Free Electron Laser (CIRFEL),<sup>8(e),8(f)</sup> which formed the design basis for the LEAF accelerator. The major LEAF accelerator system components (RF system, accelerator, beam line, controls) were built by Northrop-Grumman. Conventional construction of the LEAF facility building began in October 1994. Commissioning began in March 1997 and permission for routine operation was granted by the U. S. Department of Energy in 1998. Installation of experimental systems and accelerator upgrades has continued since then. Since the inception of the LEAF, several other photocathode-based pulse radiolysis facilities have been built, are under construction, or have been proposed, starting a worldwide renaissance of ultrafast pulse radiolysis.<sup>6(d),12–14</sup> This report describes the LEAF facility in its present state of evolution and provides information based on operational experience that other groups constructing and operating similar facilities will find useful.

## II. THE LASER-ELECTRON ACCELERATOR FACILITY

The BNL Chemistry Department's Laser-Electron Accelerator Facility (LEAF) is based around a rf photocathode accelerator expressly designed for pulse radiolysis. Compared to similar devices designed for free electron lasers and other accelerator physics applications, the key distinctions of the LEAF are higher charge per pulse (up to 20 nC) to deliver a large radiolytic dose, and an accelerator system that is easy for nonspecialists to operate at high levels of performance.

### A. Layout

The LEAF facility is located in an underground vault adjacent to the basement of the Chemistry Building at BNL. It consists of three main rooms as shown in Fig. 1: the control room (18.3 × 3 to 4.3 m), the laser room (6.7 × 6.8 m), and the accelerator vault (12.5 × 7.8 m). The laser room, which also contains the high-power pulsed rf system that powers the accelerator, sets LEAF apart from a typical pulse radiolysis facility. It is essential to be able to monitor and adjust the laser system while the accelerator is running. Therefore, the lasers are placed outside the shielded accelerator vault but as close as practical to the accelerator in order to minimize laser beam transport distances to the accelerator (~4 m) and to the optical table for laser-electron pulse coincidence experiments. The operator's control console is located in the control room in close proximity to the accelerator, the high-power rf system, and the beam transport control racks within the accelerator vault. Two experimental stations in the control room correspond to the two target areas that have been installed to date. (Provision has been

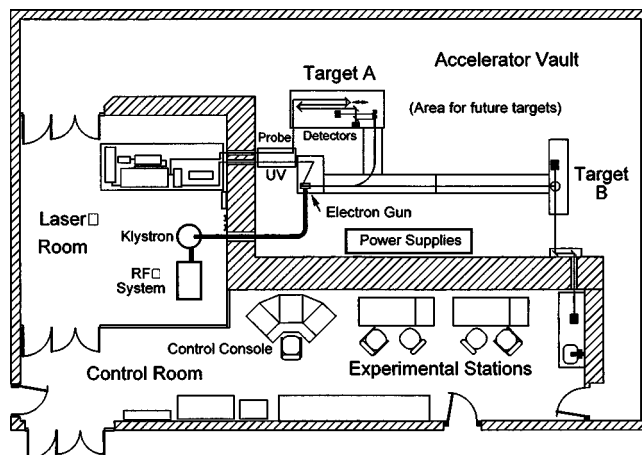


FIG. 1. Layout of the Laser-Electron Accelerator Facility.

made for further target installations between the two existing targets.) The station in the center controls the picosecond electron pulse—laser probe transient absorption experiment, while the one on the right is configured for digitizer-based transient absorption and pulse conductivity measurements.

The underground location of the LEAF facility and a tightly regulated heating and ventilation system provide the good temperature stability ( $21.7 \pm 0.6$  °C, relative humidity ~55%) essential for proper operation of the accelerator and laser systems, which require picosecond synchronization of laser pulses and microwaves over signal propagation lengths of tens of meters. Temperature excursions in excess of 1 °C can induce beam misalignments that degrade the stability of the laser system.

### B. Accelerator system

The LEAF rf photocathode electron gun accelerator is shown in Fig. 2. It is a 3.5-cell, 2856 MHz resonant cavity structure composed of OFHC copper. Each cell of the gun is fitted with a rf pick-up loop to measure the instantaneous microwave power, and a copper tuning slug mounted on a

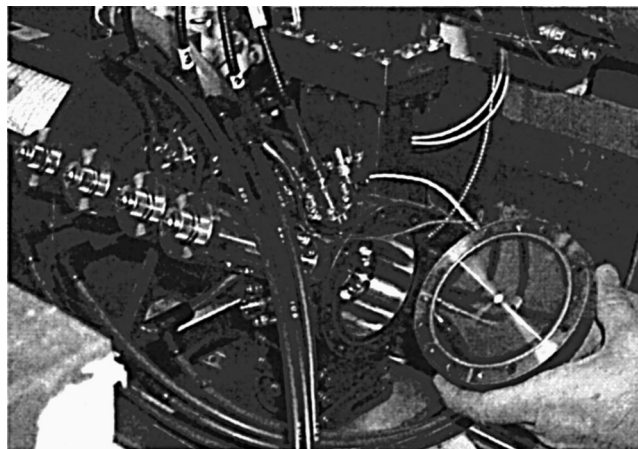


FIG. 2. Picture of the LEAF electron gun, showing the Mg photocathode on the back plate. Also visible: cooling lines above and below the tuning slug actuators (cylinders on the left), rf pickup loop feed-throughs above the tuning slugs, laser window below the first tuning slug, camera window on top of the accelerator, rf waveguide behind the camera window, solenoid magnet at left.

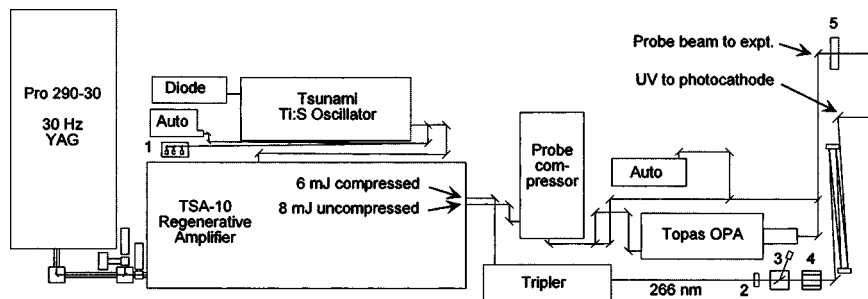


FIG. 3. Schematic of LEAF laser and optical system components. Diode: Millennia Vi Nd:YVO<sub>4</sub> CW laser. Auto: autocorrelators. 1: Oscillator diagnostic and timing pick-ups. 2: Remote-controlled rotating waveplate. 3: Thin-film polarizer and beam stop. 4: UV beam shutter with integral beam stop. 5: Probe beam shutter.

vacuum actuator. A 6 mm diameter magnesium plug is pressed into the back plate of the gun to serve as the photocathode. The back plate can be removed for resurfacing as needed; two back plates are used in rotation. A Suprasil vacuum window in the horizontal plane of the photocathode is used to introduce the 266 nm laser pulse that excites photoelectrons from the cathode. A fused silica window is mounted in the vertical plane of the cathode to serve as a viewing port for a video camera to monitor the laser spot. Both windows are aligned 65° from normal incidence with respect to the cathode surface.

Temperature control for the accelerator consists of passive external cooling from a chilled water loop and actively controlled resistive heating. The first half-cell of the accelerator and the other three cells grouped together constitute two separate temperature control zones. The operating temperature is approximately 54 °C, but the two zone set points may differ by well over a degree Celsius. The heat load due to microwave power dissipation in the accelerator varies significantly depending on the mode of operation. At present, the rate of cooling water flow is switched between two settings depending on repetition rate (1 Hz vs 10–30 Hz) but a more sophisticated system is under consideration.

Microwave power for acceleration is supplied by a standard modulator and S-band klystron assembly producing 15 MW peak power and a pulse width of 2.5 μs. The klystron presently in use is a former Stanford Linear Accelerator Center XK-5 tube. The modulator contains an 8-element pulse-forming network powered by a 6 kVA, 40 kV high voltage power supply (General Atomics, San Diego, CA) and triggered by an LS-3229 thyatron (Perkin-Elmer, Salem, MA). The microwave frequency source plays a critical role in photocathode accelerator installations because it must supply phase-synchronized signals to both the microwave amplification system and the laser system used to drive the photocathode. At the LEAF, the master reference oscillator (MITEQ XTO-02-81.6) operates at 81.6 MHz to supply the titanium sapphire oscillator laser with a reference signal for cavity length stabilization (*vide infra*). A phase-locked loop is used to generate the 35th harmonic (2856 MHz), which is amplified (Pro-Comm, PC-3000S, Brick, NJ) to 500 W before seeding the klystron. The section of S-band waveguide immediately after the klystron incorporates a microwave circulator (pressurized with SF<sub>6</sub>) for isolation, followed by a microwave window connecting to the vacuum section of waveguide leading to the gun. The waveguide contains pick-ups to measure forward and reflected microwave power for monitoring at the control console.

### C. Laser system

The work function of the magnesium metal photocathode requires UV wavelengths of 280 nm or shorter to produce photoelectrons. This is accomplished at the LEAF by frequency-tripling the 800 nm output of a 30 Hz, chirped-pulse amplified titanium sapphire (Ti:S) laser system. The key element in the laser system is the frequency-stabilized Ti:S oscillator (Spectra Physics Lok-to-Clock Tsunami). The Lok-to-Clock unit adjusts the oscillator's cavity length to match the 81.6 MHz reference frequency generated by the microwave system. This provides the synchronization for the amplified, frequency-tripled 266 nm laser pulse to consistently strike the photocathode at the correct point in the microwave cycle for proper acceleration of the photoelectrons. The timing jitter is on the order of a picosecond, which corresponds to one degree of phase at 2856 MHz.

Figure 3 shows a schematic of the laser system and optical transport components. The Tsunami Ti:S oscillator is pumped at 532 nm by a 5 W (continuous) Spectra Physics Millennia-Vi intracavity-doubled, diode-pumped Nd:YVO<sub>4</sub> laser. The 800 nm oscillator output passes into a Spectra Physics TSA-10 amplifier pumped at 532 nm by a 30 Hz Nd:YAG laser (Spectra Physics GCR-290-30 Pro). The 100 fs, 8 nJ oscillator pulses are grating-stretched to ~200 ps, regeneratively amplified to 3 mJ and amplified again to 16 mJ in two passes through a second amplifier rod. A beam-splitter directs half of the beam to a homemade external compressor, which recompresses the pulses to ≈100 fs for generation of probe beams for pulse-probe transient absorption and other experiments. The probe beam can be used at the 800 nm fundamental wavelength, doubled to 400 nm, used to drive an optical parametric amplifier (Quantronix/Light Conversion TOPAS, Hauppauge, NY) to generate tunable probe beams from 240 to 2600 nm, or used for continuum generation for wavelength-dispersed pulse-probe detection.

The other half of the amplifier output goes to the TSA-10 internal compressor, which partially compresses the pulses to 1–6 ps for input to the homemade frequency tripler that produces the 266 nm beam used to excite photoelectrons from the magnesium cathode on the back plate of the accelerator. The bandwidth of the femtosecond Ti:S system enables the UV pulse width to be tunable, which is an important control feature. A longer laser pulse width is desirable if large amounts of charge are to be extracted, normally the case in pulse radiolysis applications, since it keeps the charge density low. If the charge density is too high, space-charge

self-repulsion of the electron bunch will cause it to broaden in all directions, and the effective accelerating field gradient will be reduced by the field due to the electron bunch itself. Both of these effects limit the ability of the beam transport system to compress the electron pulse at the experimental target location. A remotely controlled waveplate and polarizer combination allows adjustment of the 266 nm pulse energy available for cathode illumination up to 0.5 mJ. The UV beam travels from the laser room to the accelerator table through a hole in the shielding wall, across some alignment and beam shaping optics and through a Suprasil window onto the photocathode. A remotely controlled turning mirror permits the operator to align the UV beam on the cathode during accelerator operation. For certain applications, an echelle grating is used to correct the laser pulse front for 65° incidence on the photocathode. Without correction, the pulse front takes 18 ps to traverse the 6 mm diameter of the magnesium button. Polarization of the UV laser pulse at the photocathode is horizontal, so that it strikes in “*p*”-incidence for maximum quantum efficiency.

#### D. Beam line

The beam transport system consists of a straight section leading to two arms (lines A and B), selected by setting the first of two 45° bending dipole magnets along the “A” line that supports the pulse-probe experiment. The electron beam emitted by the rf electron gun is collected by a solenoid magnet. Two pairs of horizontal and vertical steering dipoles center the electron beam, which is conducted down the rest of the beam line by pairs of quadrupole magnets that counteract transverse expansion due to space charge effects. Beam transport is monitored by five integrating current transformers (ICT-082, Bergoz Instrumentation, Crozet, France) positioned across electrically insulated gaps in the beam tubes at critical locations. The ICTs allow the operator to measure total charge (photocurrent and dark current) at the output of the solenoid magnet, and to monitor and optimize beam transport efficiency to the target locations. Six pneumatically actuated “pop-up” beam position monitor flags are used to determine the electron beam’s position and profile. Transition radiation is generated when the beam strikes a pop-up flag, forming an image of the beam profile that is collected by video camera (after passage through a fused silica vacuum window) and relayed to a monitor at the control console. The video image is analyzed by commercial laser beam profiling software (Sensor Physics LaserTest LS-4, Oldsmar, FL).

The vacuum system is divided into three zones separated by two pneumatic gate valves for ease of service. The gun and waveguide section is pumped by two 75 l/s ion pumps, while the A- and B-line sections have three and two 25 l/s pumps, respectively. To facilitate leak analysis and helium leak checking, a residual gas analyzer (Stanford Research Systems RGA-200, Sunnyvale, CA) is mounted on the A-line section. The pressure at various points in the system varies from 3 to  $15 \times 10^{-9}$  Torr. Although it would be desirable to have higher vacuum in the system, Viton O-rings are required as gaskets for the the back plate seal on the rf gun, insulated electrical breaks for the ICTs, and the beam win-

dow assemblies at the target stations. The beam windows are made from a single 0.5 mil (12.5  $\mu\text{m}$ ) aluminum sheet (type 1100H19) sealed against an O-ring on a 1.33 in. Conflat flange with a regular copper gasket for backing on the outer side. The beam window is designed to be as thin as possible to reduce scatter of the electron beam before striking the sample. Despite the thinness, this kind of window assembly has proved to be durable. In accelerator systems that use thermionic electron sources, loss of vacuum due to window rupture can result in significant damage and expense, however in the case of the LEAF accelerator the consequences of vacuum loss are slight. After restoration of the vacuum it may be necessary to clean the magnesium photocathode by scanning with a focused laser beam for  $\sim 20$  min, followed by an hour or two of rf conditioning before normal operation is restored.

#### E. Control system

The simplicity and user-friendliness of the LEAF control system are key advantages of this type of accelerator design. It is relatively easy for new staff members to learn to operate the LEAF accelerator proficiently, particularly in comparison to the older generation of picosecond linear accelerator pulse radiolysis facilities. There are only two operator controls for the microwave system—the microwave power applied to the accelerator and the microwave phase relative to the timing of the laser pulse on the photocathode. One oscilloscope displays the forward and reflected microwave power, along with the coarse (nanosecond) timing of the laser pulse. Two more oscilloscopes monitor microwave power in each of the four cells of the gun and signals from the integrating current transformers that measure beam current at various points along the beam line. Together, these signals permit the operator to assess whether the gun is properly tuned and whether the transport parameters are correct. Gun tuning is strongly dependent on the gun temperature, which goes through excursions from the set points when the microwave power is turned off and on (for example, when experimenters enter the vault to change radiolysis samples). The amplitude and duration of the excursion depends on the duty factor, which varies with the operating mode.

The beam transport system is automated using the National Instruments LabVIEW graphical programming environment running on a Macintosh computer, using a combination of GPIB, digital I/O and analog input cards. The beam transport system is represented graphically on the computer display as shown in Fig. 4. The software controls and monitors all of the magnet power supplies (1 solenoid, 2 bending dipoles, 8 pairs of horizontal and vertical steering dipoles, and 16 quadrupoles), two pneumatic gate valves for isolation of beam line sections, and the 6 pneumatic actuators for the pop-up beam position monitor flags. The software also displays pressure readings from ionization gauges and ion pumps on the beam line and temperatures of critical components. The control software will prevent firing of the rf modulator if it detects a vacuum failure or the loss of coolant flow through the electron gun. The operator can also use the LabVIEW-based system to control the position and intensity of the UV laser pulse on the photocathode, via a turning

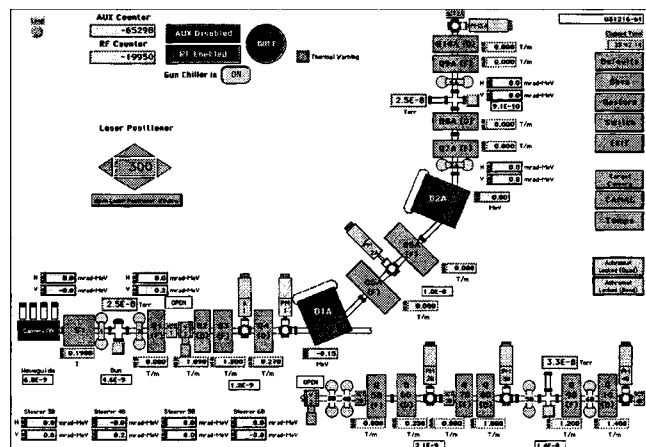


FIG. 4. "Front panel" of the LabVIEW-based accelerator control system.

mirror mount and a waveplate rotator equipped with Picomtors (New Focus, Santa Clara, CA). The software can store and recall sets of magnet settings, making daily start-up and configuration changes between targets very easy.

### F. Operation and performance

The LEAF facility is in daily service and operational reliability is high. Daily start-up involves a 1 h warm-up of the laser systems. (Earlier configurations of the laser system required longer warm-up periods.) During that time the klystron cathode comes up to temperature and the accelerator temperature control system equilibrates to the cooling water flow. Beam line control settings are recalled from the appropriate file and experimental detection systems are prepared, including alignment of the pulse-probe optics, if necessary. A brief tune-up procedure is performed to adjust the relative timing of the laser pulse and microwave phase.

There are two common operational modes for the LEAF system: 10 or 30 Hz operation for the pulse-probe transient absorption experiment at target A and single-shot operation for the digitizer-based transient absorption and conductivity experiments at target B. In either case, the amplified laser system runs constantly at 10 or 30 Hz. The microwave system runs at 5–15 Hz for pulse-probe measurements and 1 Hz for digitizer experiments. Control of accelerator "firing," i.e., acceleration of photocurrent, operates through a shutter gating the UV beam that hits the photocathode. Experiment timing is entirely controlled by the accelerator and laser systems, which are synchronized at the levels of the 60 Hz line frequency, laser Q-switch/rf modulator triggering (nanoseconds), and the picosecond-resolution laser/microwave phase control.

Typical system performance at pulse-probe target A delivers  $\geq 7$  ps-long pulses containing 6–8 nC of 8.7 MeV electrons, generating a solvated electron concentration of  $\approx 9 \mu\text{M}$  in 1 cm of water at 10 ps for a 6 nC pulse. The nominal beam diameter at the A target is 5 mm. Electron pulses at target B are nominally 10 nC and 30 Gy. The pulse width at target B has not been measured but is known from the detection limits of transient absorption measurements to be less than 120 ps. Photocurrent transport efficiency to either target exceeds 90% on the basis of ICT readings. The

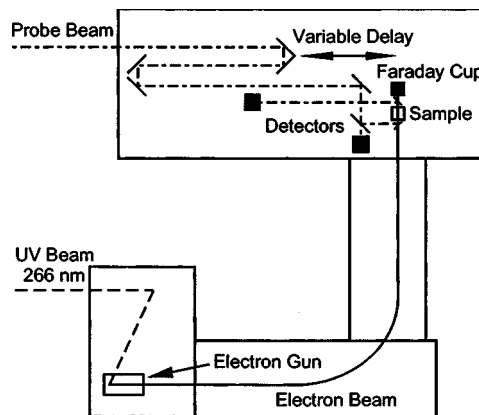


FIG. 5. Schematic of the LEAF pulse-probe detection system.

difference in photocurrent between the two targets stems from the effect of repetitive UV exposure of the Mg photocathode in the pressure regime in which the accelerator system normally operates ( $\leq 1 \times 10^8$  Torr). Under these conditions the effective quantum efficiency is highest when the photocathode is UV-pulsed at intervals of several seconds (effectively single-shot). Repetitive pulsing at the full repetition rate of the laser (as used for pulse-probe experiments) causes the quantum efficiency to decrease. The effect is less pronounced if the vacuum is higher, and its origin is unknown but probably relates to surface absorption of residual gases.

### G. Experimental systems

The A-target beam line is designed to have a short electron pulse width for picosecond electron pulse, time-delay laser probe experiments (Fig. 5), as previously described.<sup>15</sup> Probe beams of  $\sim 100$  fs duration of the 800 nm fundamental, 400 nm second harmonic, or any OPA-generated wavelength can be delayed up to 10 ns using a 1.5 m stage and Al- or Au-coated hollow corner-cube retroreflectors. The probe beam passes through a 200  $\mu\text{m}$  aperture, after which a 50:50 beamsplitter splits it into sample and reference arms. The sample beam passes through the sample ( $\leq 1$  cm pathlength) collinearly and in the same direction as the electron beam to avoid broadening the instrument response due to the two beams reaching different parts of the sample at different times. Even with the beams traveling collinearly in the same direction, broadening can occur due to the sample thickness because of the different velocities of the electron ( $\approx c$ ) and laser pulses ( $c/n$ ) in the sample, where  $c$  is the speed of light in vacuum and  $n$  is the refractive index. The sample beam is transported approximately 1.8 m before striking the photodiode to allow the Cerenkov light generated in the sample by the electron beam to diverge, reducing its effect on the absorbance measurement.

Silicon photodiodes (PIN-10D, UDT Sensors, Hawthorne, CA) are used for detection for wavelengths from 400 to 1000 nm, while InGsAs photodiodes (PDA400, ThorLabs, Newton, NJ) are used from 1000 to 1700 nm. Signals from the reference and sample photodiodes and the Faraday cup located behind the sample are digitized by a LeCroy (Chestnut Ridge, NY) 9354 oscilloscope in segment mode, trig-

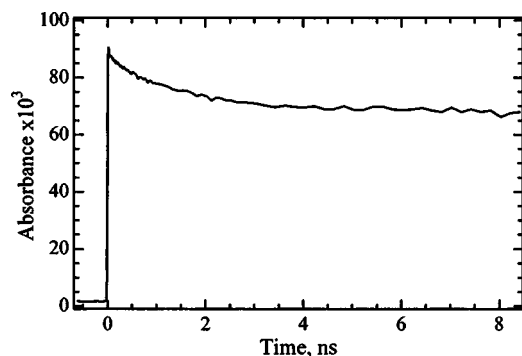


FIG. 6. Pulse-probe transient absorption data at 800 nm for argon-purged, circulated  $\text{H}_2\text{O}$  in a 1 cm flow cell. Each data point represents the average of  $18 \pm 2$  accelerator pulses. Charge per pulse was 2.5 nC, and the dose is approximately 13 Gy.

gered at the repetition rate of the laser, to collect all the measurements (typically 40–200 laser pulses) at a given delay stage position. As mentioned above, the microwave system is triggered at half the repetition rate of the laser system, so consecutive absorbance measurements alternate between electron beam on and off. Because the experiments usually require thousands of shots, 5–100 ml of sample is typically passed through a 0.4 or 1.0 cm path length Suprasil flow cell in a closed-loop system. The experiment is controlled using LabVIEW software on a Macintosh G4, which passes the data directly to custom routines running under Igor Pro software (WaveMetrics, Inc., Lake Oswego, OR) for processing and data analysis.

Figure 6 shows an example of pulse-probe transient absorption data obtained at 800 nm for the radiolysis of argon-purged, deionized (Milli-Q Plus, Millipore, Bedford, MA) water, circulated through a 1 cm path length flow system with a reservoir volume of 20 ml. The data were fit to a double exponential for the purpose of estimating the ratio of solvated electron absorbances at 10 ps (0.0895) and 10 ns (0.0683). Assuming a solvated electron yield ( $G$  value) of 3.1 per 100 eV absorbed at 10 ns,<sup>16</sup> then  $G(10 \text{ ps}) = 4.1$ , consistent with recently reported values of  $4.0 \pm 0.2$  at time zero<sup>16</sup> and  $4.1 \pm 0.2$  at 20 ps.<sup>17</sup>

Digitizer-based transient absorption and conductivity experiments are conducted at the B target. For the absorption measurements, detection light is provided by a 75 W pulsed xenon arc lamp in an ellipsoidal reflector housing (Photon Technology International, Laurenceville, NJ). The analyzing light is propagated through the sample ( $\leq 2$  cm path length) collinearly but opposite in direction to the electron beam to minimize collection of Cerenkov light. The analyzing light is then transported by lenses and mirrors to a detector in the control room to avoid detector spikes from electrical noise and x-ray hits, as well as providing for detection flexibility without shutting the accelerator system off. The optical transport system is also optimized to avoid bandwidth limitation and noise pickup by keeping the signal cable between the detector and digitizer as short as possible. Narrow (10 nm) and wide (40 nm) bandpass filters are used to select the analyzing wavelength from the UV to the NIR. Several types of photodiode (Si, Ge, InGaAs) and biplanar phototube (Hamamatsu R1328U) detectors are used depending on the

desired wavelength and time resolution. Available digitizers include Tektronix (Beaverton, OR) TDS-680B and TDS-694C oscilloscopes, SCD 5000 and 7250 scan conversion digitizers, and a LeCroy Wavemaster 8600 oscilloscope, the latter two units having 6 GHz bandwidth. Signal rise times as short as 120 ps have been measured using the phototube/7250 combination. A Faraday cup within the sample holder intercepts the electron pulse after it has passed through the sample so that the absorbance measurements can be normalized for dose. Samples are usually contained in Suprasil spectrophotometer cuvettes or cylindrical cells up to 2 cm in length. Sample temperature control is achieved using a water-jacketed cell holder, or for lower temperatures, a thermostated cell holder cooled by liquid nitrogen boil-off. Experimental hardware is controlled and data is collected using custom software running on a DEC VAXstation 4000 computer or on a Macintosh G4 running LabView. Both Fortran code on the VAX and customized Igor Pro software are used to process and analyze the data.

Excess electron mobilities and reactions in nonpolar and supercritical solvents are measured by transient conductivity at the LEAF B target. The experimental apparatus has been described previously.<sup>18</sup> For these experiments samples are irradiated using Bremsstrahlung x rays from the electron beam stopping in the Faraday cup of the transient absorption cell holder. Typical doses are less than 10  $\mu\text{Gy}$ . The current signal is amplified with a current to voltage converter before being fed to a LeCroy 9362 oscilloscope.

## H. Operating experience

The modulator and laser systems were originally designed to operate at repetition rates up to 10 Hz. Early experience with the pulse-probe acquisition system using (100–200 electron pulses per data point) indicated that the time required to collect data could be considerably reduced by increasing the repetition rate of both systems. A 30 Hz Nd:YAG pump laser and a larger modulator power supply were installed to upgrade the system repetition rate to 30 Hz. Concurrently, various improvements in the pulse-probe detection system reduced the typical number of shots required per data point by a factor of 5–10. Presently, translation stage movement and data manipulation take longer per point than data collection, although installation of a faster translation stage would remove this limitation. A potentially more significant limitation is the deactivating effect of repetitive UV laser pulses on the photocathode. Typically, a pause of several seconds before data collection at each stage position is used to allow cathode efficiency to recover. Hence, a further increase in repetition rate would only be marginally beneficial for pulse-probe measurements. Furthermore, other elements of the modulator and rf system would need to be modified or replaced to meet the higher power dissipation requirements of the increased power input. Temperature control and tuning of the rf photocathode electron gun itself becomes more difficult as the repetition rate increases and the differences in operating conditions between low- and high-repetition rate modes get larger. Operation at higher repetition rates would be aided by a more sophisticated temperature control system that dynamically controls cooling

water flow as well as the resistive heating elements. A final but significant consideration concerning system repetition rate is the fact that the lamp-pulsed Nd:YAG amplifier pump laser must be run at the full repetition rate at all times even if the facility is being used for single-shot digitizer-based experiments, which represent a substantial portion of the operational schedule. A higher repetition rate requires more frequent replacement of consumables such as flashlamps, resulting in greater operating expense, as well as accelerated wear on laser system components that may have an impact on reliability.

### III. APPLICATIONS

The BNL Center for Radiation Chemistry Research (CRCR) consists of three radiolysis facilities: LEAF, a 40-ns minimum pulse width 2 MeV electron Van de Graaff accelerator with transient absorption and conductivity detection, and a 5 kGy/h  $^{60}\text{Co}$  gamma source. Operations at LEAF concentrate on experiments that require higher time resolution, higher beam energy, and the availability of synchronized laser pulses. LEAF's pulse-probe absorption system was used to observe the formation of  $\text{Xe}_2^*$  excimers in irradiated supercritical xenon (scXe) and rates of electron attachment to  $\text{C}_6\text{F}_6$  in scXe and subsequent electron transfer to benzoquinone were also measured at the digitizer-based experimental station.<sup>18</sup> LEAF has been used to investigate fast electron transfer reactions in dendrimers<sup>19</sup> and molecular wires.<sup>20</sup> Measurements of solvated electron spectra in ionic liquids and kinetic studies of solvated and presolvated ("dry") electrons and of H-atoms in these unique media have also been made at LEAF.<sup>21</sup> The conductivity detection system has been used to determine rates of electron attachment to several solutes in supercritical ethane and to  $\text{C}_{60}$  in several solvents.<sup>22</sup> Digitizer-based experiments at LEAF demonstrated that addition of arenes such as benzene or toluene increased the yield of radical cations in irradiated dichloroethane.<sup>23</sup> Ongoing studies include geminate recombination and electron-hole pair distribution in aliphatic and aromatic nonpolar solvents, picosecond dissociation of aryl-halide molecules upon electron attachment,<sup>24</sup> "dry" electron capture, excited states of radical ions, and further work on ionic liquids, molecular wires, electron transfer and nanoscience applications. Access to the LEAF facility by users outside of BNL is encouraged, either through collaboration with BNL staff or via user-facility arrangements. Please contact the authors (wishart@bnl.gov, acook@bnl.gov, jrmiller@bnl.gov) or the general user facility address (crcr@bnl.gov) for more information.

### ACKNOWLEDGMENTS

The authors wish to thank Stephen Howell, Harold Schwarz, Edward Castner, Richard Holroyd, Norman Sutin, Pavel Poliakov, J. P. Kirby, Alison Funston, Sergei Lyman, James Anselmini, Kenneth Batchelor, Joseph Sheehan, Ilan Ben Zvi, Xijie Wang, John Axe (all BNL); Ira Lehrman (Northrop-Grumman); Hans Bluem, Vincent Christina, Jack Ditta, Richard Hartley (Advanced Energy Systems); Alan Del Gaudio and Joseph Juenemann (Spectra Physics); Robert

Ettlebrick and David Kemp (Positive Light); for contributions to the planning, construction and operation of the LEAF facility. This work was carried out at Brookhaven National Laboratory under Contract No. DE-AC02-98CH10886 with the U.S. Department of Energy and supported by its Division of Chemical Sciences, Office of Basic Energy Sciences. Support from the BNL LDRD Program (Project No. 97-29) is acknowledged. The authors thank Professor Yosuke Katsumura for the preprint on solvated electron yield in water.

- <sup>1</sup>(a) *Radiation Chemistry: Present Status and Future Trends*, edited by C. D. Jonah and B. S. M. Rao (Elsevier Science, New York, 2001), Vol. 87; (b) *Radiation Chemistry: Principles and Applications*, edited by Farhataziz and M. A. J. Rodgers (VCH Publishers, New York, 1987); (c) *Properties and Reactions of Radiation Induced Transients*, edited by J. Mayer (Polish Scientific Publishers PWN, Warsaw, 1999); (d) A. R. Denaro and G. G. Jayson, *Fundamentals of Radiation Chemistry* (Butterworth, London, 1972); (e) *Pulse Radiolysis*, edited by M. Ebert, J. P. Keene, A. J. Swallow, and J. H. Baxendale (Academic, New York, 1965).
- <sup>2</sup>J. F. Wishart, in *Photochemistry and Radiation Chemistry: Complementary Methods for the Study of Electron Transfer*, edited by J. F. Wishart and D. G. Nocera, Adv. Chem Ser. 254 (American Chemical Society, Washington, D.C., 1998), Chap. 3.
- <sup>3</sup>(a) M. J. Bronskill and J. W. Hunt, J. Phys. Chem. **72**, 3762 (1968); (b) M. J. Bronskill, W. B. Taylor, R. K. Wolff, and J. W. Hunt, Rev. Sci. Instrum. **41**, 333 (1970); (c) C. D. Jonah, *ibid.* **46**, 62 (1975).
- <sup>4</sup>(a) H. Kobayashi, T. Ueda, T. Kobayashi, S. Tagawa, and Y. Tabata, Nucl. Instrum. Methods **179**, 223 (1981); (b) Y. Tabata, H. Kobayashi, M. Washio, S. Tagawa, and Y. Yoshida, Radiat. Phys. Chem. **26**, 5 (1985); (c) H. Kobayashi, Y. Tabata, T. Ueda, and T. Kobayashi, Nucl. Instrum. Methods Phys. Res. B **24/25**, 1073 (1987).
- <sup>5</sup>S. Takeda, K. Tsumori, N. Kimura, T. Yamamoto, T. Hori, T. Sawai, J. Ohkuma, S. Takamuku, T. Okada, K. Hayashi, and M. Kawanishi, IEEE Trans. Nucl. Sci. **NS-32**, 3219 (1985).
- <sup>6</sup>(a) G. Mavrogenes, J. Norem, and J. Simpson, in *Proceedings of the 1986 Stanford Linear Accelerator Conference*, Stanford Linear Accelerator Center Report No. SLAC-0303, Stanford, CA, pp. 429-430; (b) G. L. Cox, D. W. Ficht, C. D. Jonah, G. S. Mavrogenes, and M. C. Sauer, Jr., in *Proceedings of the 1989 IEEE Particle Accelerator Conference* (IEEE, Piscataway, NJ, 1989), pp. 912-914; (c) M. Uesaka, T. Ueda, T. Kozawa, and T. Kobayashi, Nucl. Instrum. Methods Phys. Res. A **406**, 371 (1998); (d) M. Uesaka, K. Kinoshita, T. Watanabe, T. Ueda, K. Yoshii, H. Harano, K. Nakajima, A. Ogata, F. Sakai, H. Kotaki, M. Kando, H. Dewa, S. Kondo, Y. Shibata, K. Ishi, and M. Ikezawa, *ibid.* **410**, 424 (1998); (e) T. Kozawa, Y. Mizutani, K. Yokoyama, S. Okuda, Y. Yoshida, and S. Tagawa, *ibid.* **429**, 471 (1999); (f) T. Kozawa, Y. Mizutani, M. Miki, T. Yamamoto, S. Suemine, Y. Yoshida, and S. Tagawa, *ibid.* **440**, 251 (2000).
- <sup>7</sup>L. H. Luthjens, M. J. W. Vermeulen, and M. L. Horn, Rev. Sci. Instrum. **51**, 1183 (1980).
- <sup>8</sup>(a) K. Batchelor, I. Ben-Zvi, R. C. Fernow, J. Fischer, A. S. Fisher, J. Gallardo, G. Ingold, H. Kirk, L. Lin, R. Malone, K. McDonald, I. Pogorelsky, D. Russel, T. Srinivasan-Rao, J. T. Rogers, J. F. Sheehan, T. Tsang, J. Sheehan, S. Ulc, X. J. Wang, M. Woodle, J. Xie, and R. Zhang, Nucl. Instrum. Methods Phys. Res. A **318**, 372 (1992); (b) I. S. Lehrman, I. A. Birnbaum, S. Z. Fixler, R. L. Heuer, S. Siddiqi, I. Ben-Zvi, K. Batchelor, J. C. Gallardo, H. G. Kirk, and T. Srinivasan-Rao, *ibid.* **318**, 247 (1992); (c) X. J. Wang, T. Srinivasan, K. Batchelor, M. Babzien, I. Ben-Zvi, R. Malone, I. Pogorelsky, X. Qiu, J. Skaritka, and J. Sheehan, *ibid.* **375**, 82 (1996); (d) X. J. Wang, in *Proceedings of the 2001 Particle Accelerator Conference, Chicago, IL, June 18-22, 2001*, <http://accelconf.web.cern.ch/accelconf/p01/PAPERS/MOPB008.PDF>; (e) S. J. Russell, Nucl. Instrum. Methods Phys. Res. A **507**, 304 (2003); (f) J. Krishnaswamy, I. S. Lehrman, J. Sheehan, R. L. Heuer, M. F. Reusch, and R. Hartley, in *Proceedings of the 1993 Particle Accelerator Conference, Washington, D.C., May 17-20, 1993* (IEEE, Piscataway, NJ, 1993), pp. 1527-1529; (g) I. S. Lehrman *et al.* Proc. SPIE **2522**, 451 (1995).
- <sup>9</sup>A rf photocathode injector has replaced the prebunching system on one of the two linear accelerators at NERL [Ref. 6(d)].
- <sup>10</sup>The World Wide Web Virtual Library: Free Electron Laser Research and Applications. [http://sbfel3.ucsb.edu/www/vl\\_fel.html](http://sbfel3.ucsb.edu/www/vl_fel.html).

- <sup>11</sup>C. Creutz, H. A. Schwarz, and J. F. Wishart, "Report of the Workshop on the Proposed Pulse Radiolysis Facility at Brookhaven National Laboratory," BNL Report, BNL-52229 (1989).
- <sup>12</sup>Y. Muroya, M. Lin, T. Watanabe, T. Kobayashi, G. Wu, T. Ueda, K. Yoshii, M. Uesaka, and Y. Katsumura, Nucl. Instrum. Methods Phys. Res. A **489**, 554 (2002).
- <sup>13</sup>(a) J. Belloni, M. Gaillard, H. Monard, M. Mostafavi, I. Lampre, H. Remita, J. L. Marignier, J. C. Bourdon, and T. Garvey, J. Phys. IV **108**, 243 (2003); (b) T. Garvey, M. Bernard, H. Borie, J. C. Bourdon, B. Jacquemard, B. Leblond, P. Lepercq, M. Omeich, M. Roch, J. Rodier, and R. Roux, in *Proceedings of the 2002 European Particle Accelerator Conference, Paris, France, June 3–7, 2002*, <http://accelconf.web.cern.ch/AccelConf/e02/PAPERS/THBLA003.pdf>.
- <sup>14</sup>(a) S. Kashiwagi, Y. Hama, H. Ishikawa, H. Kawai, M. Kobayashi, R. Kuroda, K. Maeda, M. Mori, F. Nagasawa, M. Washio, A. Yada, I. Ben-Zvi, X. J. Wang, H. Hayano, and J. Urakawa, in *Proceedings of the 2002 European Particle Accelerator Conference, Paris, France, June 3–7, 2002*, <http://accelconf.web.cern.ch/AccelConf/e02/PAPERS/TUPRI077.pdf>; (b) Y. Aoki, J. Yang, M. Hirose, F. Sakai, A. Tsunemi, M. Yorozu, Y. Okada, A. Endo, X. Wang, and I. Ben-Zvi, Nucl. Instrum. Methods Phys. Res. A **455**, 99 (2000).
- <sup>15</sup>J. F. Wishart, in *Radiation Chemistry: Present Status and Future Trends*, edited by C. D. Jonah and B. S. M. Rao (Elsevier Science, Amsterdam, 2001), Vol. 87, pp. 21–35.
- <sup>16</sup>D. M. Bartels, A. R. Cook, M. Mudaliar, and C. D. Jonah, J. Phys. Chem. A **104**, 1686 (2000) G-value estimate obtained from Fig. 5 of this reference.
- <sup>17</sup>Y. Muroya, M. Lin, G. Wu, H. Iijima, K. Yoshii, T. Ueda, H. Kudo, and Y. Katsumura, Radiat. Phys. Chem. (in press).
- <sup>18</sup>R. Holroyd, J. F. Wishart, M. Nishikawa, and K. Itoh, J. Phys. Chem. B **107**, 7281 (2003).
- <sup>19</sup>T. H. Ghaddar, J. F. Wishart, J. P. Kirby, J. K. Whitesell, and M. A. Fox, J. Am. Chem. Soc. **123**, 12832 (2001).
- <sup>20</sup>A. M. Funston, E. E. Silverman, J. R. Miller, and K. S. Schanze, J. Phys. Chem. B **108**, 1544 (2004).
- <sup>21</sup>(a) J. F. Wishart and P. Neta, J. Phys. Chem. B **107**, 7261 (2003); (b) J. Grodkowski, P. Neta, and J. F. Wishart, J. Phys. Chem. A **107**, 9794 (2003); (c) J. F. Wishart, S. I. Lall-Ramnarine, R. Raju, A. Scumpia, S. Bellevue, R. Ragbir, and R. Engel, Radiat. Phys. Chem. (in press); (d) J. F. Wishart, in *Ionic Liquids as Green Solvents: Progress and Prospects*, edited by R. D. Rogers and K. R. Seddon, ACS Symp. Ser. 856 (American Chemical Society, Washington, D.C., 2003), Chap. 31, pp. 381–396; (e) A. M. Funston and J. F. Wishart, in *Ionic Liquids: Progress and Prospects*, edited by R. D. Rogers and K. R. Seddon (ACS Symp. Ser., in press).
- <sup>22</sup>(a) M. Nishikawa, K. Itoh, and R. A. Holroyd, J. Phys. Chem. A **103**, 550 (1999); (b) R. A. Holroyd, M. Nishikawa, and K. Itoh, J. Phys. Chem. B **103**, 9205 (1999); (c) **104**, 11585 (2000); (d) R. A. Holroyd, K. Itoh, and M. Nishikawa, J. Chem. Phys. **118**, 706 (2003); (e) R. A. Holroyd, Radiat. Phys. Chem. (in press).
- <sup>23</sup>A. M. Funston and J. R. Miller, Radiat. Phys. Chem. (in press).
- <sup>24</sup>N. Takeda, P. V. Poliakov, A. R. Cook, and J. R. Miller, J. Am. Chem. Soc. **126**, 4301 (2004).